Tunable Optical Gap at a Fixed Lattice Constant in Group-IV Semiconductor Alloys

V. R. D'Costa,[1,*] Y.-Y. Fang,[2,†] J. Tolle,[2,‡] J. Kouvetakis,[2,§] and J. Menéndez[1,‖]

[1]*Department of Physics, Arizona State University, Tempe, Arizona 85287-1504, USA*

[2]*Department of Chemistry and Biochemistry, Arizona State University, Tempe, Arizona 85287-1604, USA*

(Received 9 September 2008; revised manuscript received 15 January 2009; published 13 March 2009)

A direct absorption edge tunable between 0.8 and ~1.4 eV is demonstrated in strain-free ternary $Ge_{1-x-y}Si_xSn_y$ alloys epitaxially grown on Ge-buffered Si. This decoupling of electronic structure and lattice parameter—unprecedented in group-IV alloys—opens up new possibilities in silicon photonics, particularly in the field of photovoltaics. The compositional dependence of the direct band gap in $Ge_{1-x-y}Si_xSn_y$ exhibits a nonmonotonic behavior that is explained in terms of coexisting small and giant bowing parameters in the two-dimensional compositional space.

DOI: 10.1103/PhysRevLett.102.107403 PACS numbers: 78.20.Ci, 71.15.Ap, 78.40.Fy, 78.66.Db

The properties of most semiconductor alloys can be understood in terms of simple interpolations between the corresponding end compounds. This is justified theoretically by the so-called "virtual crystal approximation" (VCA), which describes the alloy as a perfect crystal made of imaginary average "atoms" [1,2]. The validity of a VCA-like description means that the electronic properties (band gaps, effective masses, etc.) can be tailored to specific applications by adjusting the alloy composition. Complications arise when the alloy is grown epitaxially on a substrate, and the change in lattice constant produced by alloying must be accommodated by elastic deformation. This strain adds considerable complexity to band structure engineering and must be kept below well-defined limits to prevent the generation of misfit dislocations. In the case of III-V compounds, these complications can be largely eliminated by introducing quaternary or pseudoternary alloys which effectively decouple strain and composition [3].

$Ge_{1-x}Si_x$ alloys are nearly perfect virtual crystals with a tunable band structure that evolves smoothly from Si to Ge. The alloys grow epitaxially on Si, and the ease of fabrication and low cost of the Si substrates have fueled efforts to replace III-V materials with $Ge_{1-x}Si_x$ alloys of comparable functionality [4]. Significant progress has been made for the past two decades, but a major stumbling block is still in place: the lattice mismatch between Si and Ge exceeds 4%, and the associated large strain effects are difficult to manage. As in the case of III-V alloys, it is natural to expect that the decoupling of strain and band structure can be achieved via ternary alloys with two compositional degrees of freedom, but so far a complete decoupling has not been achieved experimentally. $Ge_{1-x-y}Si_xC_y$ alloys represent the first system to be explored for this purpose [5]. However, the solubility of C in $Ge_{1-x}Si_x$ is very limited, and the perturbation represented by the C atoms is so large that the electronic structure is no longer amenable to a VCA-like description. More recently, $Ge_{1-x-y}Si_xSn_y$ alloys with large Sn atomic fractions were introduced [6]. These alloys represent the first realistic opportunity for independent strain and band structure manipulation. Results so far demonstrate a linear compositional behavior of the average lattice constant [7] and high-energy interband transitions that depend on both x and y [7,8].

In this Letter we show experimentally that a full decoupling of lattice constant and band structure can be achieved in $Ge_{1-x-y}Si_xSn_y$ alloys lattice-matched to Ge. We study the compositional dependence of the lowest direct gap in these alloys and we find qualitative differences with one-dimensional alloys. The latter can be classified according to the magnitude of their bowing parameters (quadratic coefficients in the compositional dependence of the gap energies) into systems with moderate or low bowing, commonly characterized by extended band-edge states, and those with large or giant bowing associated with impurity-like electronic states [9]. Our $Ge_{1-x-y}Si_xSn_y$ alloys show evidence for a mixed behavior in which small and large bowing parameters are required to express the band-gap energy in terms of two-dimensional polynomials.

The growth process starts with a newly developed Ge-on-Si chemical vapor deposition (CVD) method [10] which makes it possible to deposit Ge layers on Si substrates at 350 °C. These Ge layers, with thicknesses ranging from 200 to 500 nm, exhibit strain-relaxed microstructures, very low defect densities ($\sim 10^5$ cm^{-2}), and atomically flat surfaces, thus providing an ideal platform for the subsequent growth of $Ge_{1-x-y}Si_xSn_y$ alloys. In previous work [6,7], the ternary alloy was grown on $Ge_{1-y}Sn_y$-buffered Si using the SnD_4 and $SiGeH_6$/$SiGe_2H_8$ CVD precursors. This leads to Si-concentration values $x \geq 0.2$. For this work, we need to access the $0.05 < x < 0.2$ range and fine-tune the concentrations. We discovered that this can be achieved by introducing Ge_2H_6 (digermane), and Si_3H_8 (trisilane) as additional sources of Ge and Si atoms. For low Sn concentrations ($y \sim 0.02$), ternary films can be grown at 350 °C using SnD_4, Ge_2H_6, and Si_3H_8. This bypasses the need for $SiGeH_6$ or $SiGe_2H_8$. For $y \geq 0.05$, the growth temperature must be lowered to 300–330 °C. Under these conditions the reactivity of tri-

silane is reduced, and growth of the ternary is achieved using $SiGeH_6$, with trisilane used to fine-tune the composition. A detailed account of this fascinating chemistry will be reported elsewhere.

The GeSiSn layers, ranging in thickness from 70 to 200 nm, were studied with an array of structural characterization techniques, including cross-sectional transmission electron microscopy (XTEM), Rutherford backscattering (RBS) and x-ray diffraction (XRD). Figure 1(a) shows a reciprocal space map for the (224) x-ray reflection from a $Ge_{0.90}Si_{0.08}Sn_{0.02}/Ge/Si$ sample. The inset shows a (004) scan. Notice the perfect overlap between the Ge and GeSiSn contributions. The alignment of the (224) Si and Ge/GeSiSn reflections along the reciprocal space vector direction indicates full strain relaxation in the films. Figures 1(b) and 1(c) show XTEM data confirming the high structural quality of the films.

Optical studies were carried out using a variable-angle spectroscopic ellipsometer [11] with a computer-controlled compensator. The samples were modeled as a four-layer system containing a Si substrate, the Ge buffer layer, the GeSiSn film, and a surface layer. The ellipsometric data were processed as described in Ref. [12]. This approach yields a "point-by-point" dielectric function, generated by fitting the ellipsometric angles at each wavelength to expressions containing the real and imaginary parts of the GeSiSn dielectric function as adjustable parameters, and also a parametric dielectric function obtained from a global fit to the layer thicknesses and ellipsometric angles at all wavelengths. This fit uses parametrized functional expressions for the dielectric function of tetrahedral semiconductors as developed by Johs and Herzinger (JH) [13]. The JH expressions contain many adjustable parameters, some of which are associated with critical points in the joint electronic density of states. We find that the two approaches are in excellent agreement, indirectly confirming the Kramers-Kronig consistency of the point-by-point fits. In Fig. 2 we show the imaginary part of the JH-dielectric function for representative samples. It is clear from the figure that the absorption edge can be displaced to energies higher than that of pure Ge while keeping the lattice parameter perfectly matched to Ge. Since Vegard's law is a very good approximation for GeSiSn alloys [7], the compositional formula for an alloy lattice matched to Ge is $Ge_{1-X}(Si_\beta Sn_{1-\beta})_X$, with $\beta = 0.79$. Assuming that the band-gap dependence on composition is also linear, we predict for $Si_\beta Sn_{1-\beta}$ a direct band gap $E_0 = 3.14$ eV, much larger than $E_0 = 0.80$ eV for pure Ge. Thus the band-gap increase as a function of X is to be expected.

For an in-depth analysis of the GeSiSn electronic structure we must extract precise E_0 values from experiment. The standard approach to obtain optical transition energies from ellipsometric data is to compute numerical high-order derivatives of the "point-by-point" dielectric function. This method is difficult to implement in our case because the data are quite noisy near the lowest direct gap E_0. Instead, we first extract E_0 directly from the parameters in the JH model. This is a somewhat risky approach (in spite of the excellent agreement with the point-by-point dielectric function) because the values of E_0 so obtained

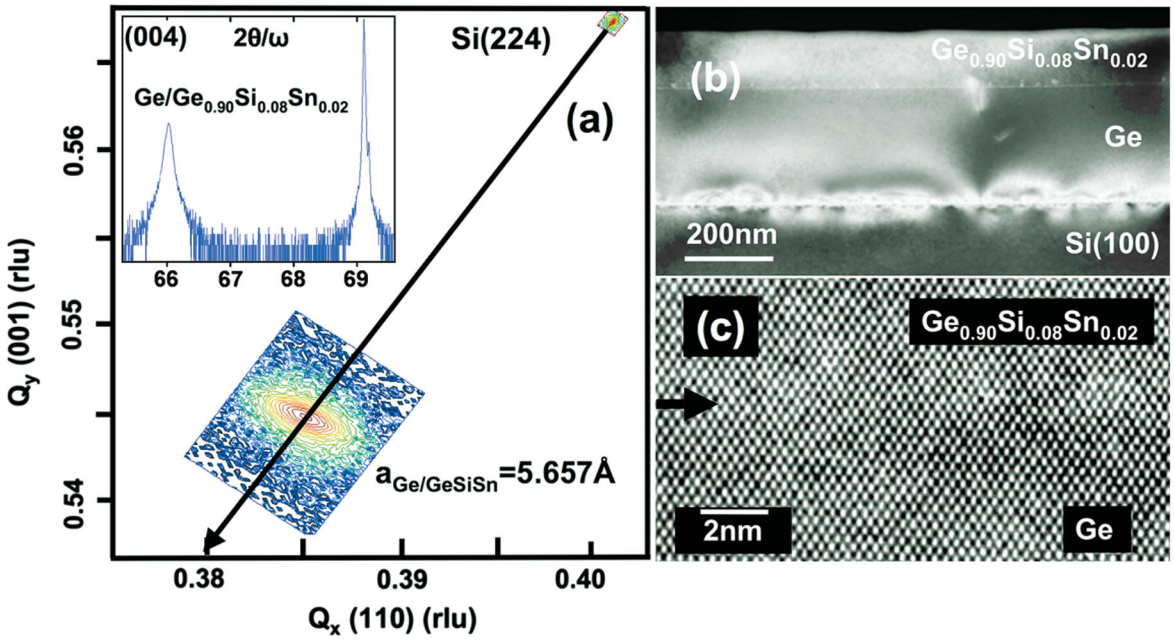

FIG. 1 (color). (a) Reciprocal space map for the (224) x-ray reflection from a $Ge_{0.90}Si_{0.08}Sn_{0.02}/Ge/Si$ sample. The Ge and GeSiSn contributions appear as a single peak due to their overlap. The overlap is also apparent in the inset showing a (004) scan. Both layers are relaxed, as confirmed by the alignment of the Si and Ge/GeSiSn reflections along the (224) reciprocal space vector direction. (b) Bright field XTEM micrograph of the entire Ge/GeSiSn film structure on Si (001). (c) High resolution XTEM image of the Ge/GeSiSn interface.

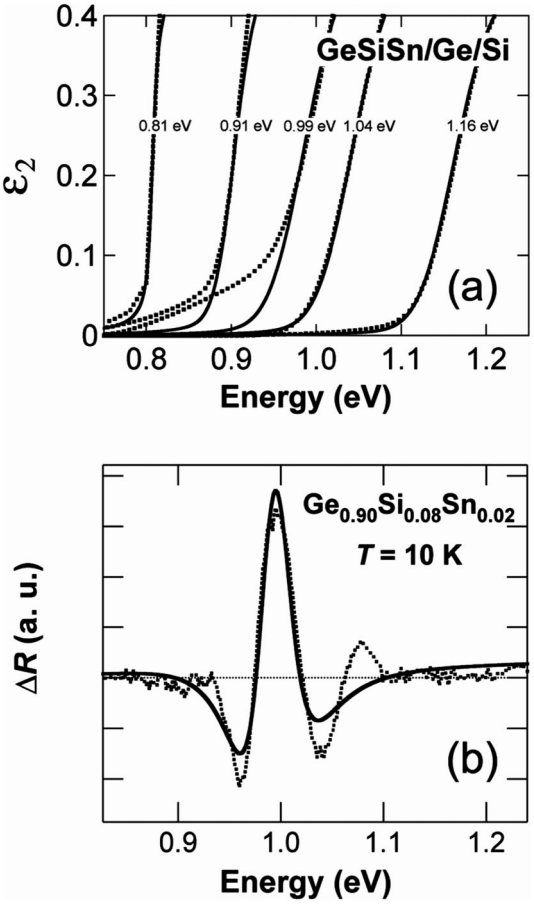

FIG. 2. (a) Imaginary part of the dielectric function of selected GeSiSn samples in the spectral region corresponding to the direct gap E_0. The dotted lines indicate the values obtained from the room-temperature spectroscopic ellipsometry data. The solid lines show fits with theoretical expressions including excitonic effects and broadening, as discussed in the text. (b) Typical low-temperature photoreflectance spectrum used to confirm the direct-gap values obtained from the ellipsometry study. The dotted line corresponds to the experimental data and the solid line is a fit using a three-dimensional critical point minimum and a Lorentzian excitonic contribution with a fixed binding energy of 4.6 meV.

could be affected by uncontrollable systematic errors due to the presence in the JH model [13] of many additional parameters with unclear physical meaning. Thus we use a second approach for the determination of E_0. Regardless of the physical meaning of its individual parameters, the JH-dielectric function can be regarded as a smooth fit of the point-by-point data with a function that is Kramers-Kronig consistent. We then fit the imaginary part of the JH-dielectric function with a realistic expression for the band-edge absorption near the E_0 gap, including excitonic effects and $\boldsymbol{k} \cdot \boldsymbol{p}$ expressions for the effective masses. The only adjustable parameters of the fit are the E_0 value and phenomenological broadening parameters. For the case of pure Ge, a Lorentzian broadening is used; for the ternary alloy we use a Voigt broadening in which the Lorentzian component is fixed and equal to that of Ge. Some of these fits are shown in Fig. 2(a). Since our expressions assume parabolic bands, they are valid only very close to the band edge, but their range of validity is sufficient to fit the E_0 values. As a third way to confirm our E_0 values, we performed photoreflectance experiments on selected samples. An example is shown in Fig. 2(b). This technique reveals sharp features corresponding to the E_0 transition. The data are modeled as a combination of a 3D critical point and an excitonic oscillator. The E_0 gap values as a function of temperature merge nicely with those found from ellipsometry. The good agreement between our three methods confirms that our E_0 values are reliable. They are shown in Fig. 3 as a function of X and compared with the linear interpolation discussed above. It is apparent that there is a strong deviation from the simple prediction, indicating the presence of large nonlinear terms in the compositional dependence of E_0.

The simplest phenomenological model beyond linear interpolation assumes that the optical transition energies in $Ge_{1-x-y}Si_xSn_y$ can be written as two-dimensional quadratic polynomials. For the E_0 gap, the corresponding expression is $E_0 = E_0^{Ge}z + E_0^{Si}x + E_0^{Sn}y - b^{GeSi}xz - b^{GeSn}yz - b^{SiSn}xy$, where $z = 1 - x - y$, E_0^{Ge} (E_0^{Si}, E_0^{Sn}) is the direct band gap in pure Ge (Si, α-Sn), and b^{GeSi} (b^{GeSn}, b^{SiSn}) is the bowing parameter of the E_0 transition in binary Ge-Si (Ge-Sn, Si-Sn) alloys. Notice that at this level of approximation the nonlinear behavior in the ternary alloy is fully determined by the nonlinear terms in the underlying binary alloys. For $Ge_{1-x-y}Si_xSn_y$ lattice matched to Ge, the band-gap expression can be rewritten as

$$E_0(X) = E_0^{Ge} + AX + BX^2 \quad (1)$$

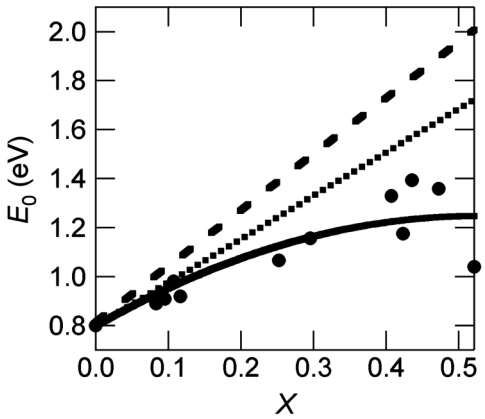

FIG. 3. Direct-gap values in GeSiSn alloys lattice-matched to Ge as a function of the combined Si + Sn fraction X. The markers correspond to the experimental values. The dashed line indicates a linear interpolation between Si, Ge, and α-Sn. The dotted line shows the linear term in the quadratic expression for the band-gap energy [Eq. (1)] as predicted from experiments on GeSn and SiGe alloys (Ref. [12]). The solid line is a fit with Eq. (1) using the linear and quadratic coefficients as adjustable parameters.

with

$$A = E_0^{\mathrm{Si}}\beta + E_0^{\mathrm{Sn}}(1-\beta) - E_0^{\mathrm{Ge}} - b^{\mathrm{GeSi}}\beta - b^{\mathrm{GeSn}}(1-\beta) \quad (2)$$

and

$$B = b^{\mathrm{GeSi}}\beta + b^{\mathrm{GeSn}}(1-\beta) - b^{\mathrm{SiSn}}\beta(1-\beta) \quad (3)$$

The linear coefficient A is determined by the elemental semiconductor band gaps and by the bowing parameters for GeSn and SiGe alloys. From Ref. [12], we obtain $A = 1.75$ eV. The linear term is plotted in Fig. 4 of that reference as a dotted line, and it is seen that it is in better agreement with experiment than the simple linear interpolation (shown by dashed line), but it still overestimates the observed E_0 values. This implies that B is negative, and from Eq. (3) we conclude that $b^{\mathrm{SiSn}} > 3.4$ eV. If we fit the band-gap values with Eq. (1), using A and B as adjustable parameters, we obtain $A = 1.70 \pm 0.42$, in excellent agreement with our prediction, and $B = -1.62 \pm 0.96$, which implies a very large $b^{\mathrm{SiSn}} = 13.2$ eV. Of course, this conclusion depends on our assumption that the compositional dependence of the band gap is quadratic. It is in principle possible that the large bowing arises from higher-order terms. For example, a large contribution proportional to xyz, which vanishes for the binary alloys, could be the explanation for the negative B. However, there are reasons to believe that a large b^{SiSn} makes a significant contribution to the quadratic coefficient B. Calculations for binary $Si_{1-y}Sn_y$ alloys [14] show a large and compositional dependent bowing parameter, ranging from $b^{\mathrm{SiSn}} = 14$ eV for $y = 0.2$ to $b^{\mathrm{SiSn}} = 4$ eV for $y = 0.5$. Previous results on the compositional dependence of the E_1 transition in GeSiSn alloys could be explained by assuming that the bowing parameters for the binary Si-Ge, Ge-Sn, and Si-Sn alloys scale according to the lattice constant and Phillips electronegativity mismatch [8]. For the E_0 transition, we have [12] $b^{\mathrm{SiGe}} = 0.21$ and $b^{\mathrm{GeSn}} = 1.94$ eV, from which we predict $b^{\mathrm{SiSn}} = 3.26$ eV. This is comparable to the value $b^{\mathrm{SiSn}} = 4$ eV for $y = 0.5$ found from supercell calculations [14]. The corresponding band edge states show considerable dispersion and do not appear to be impurity-like. We conjecture that the much higher bowing found for $y = 0.2$ signals the transition to an impuritylike regime associated with more localized states. This behavior is similar to that computed for $GaAs_{1-x}N_x$ compounds by Wei and Zunger [15], who invoked the localized character of the conduction band wave functions to explain the origin of anomalous bowing behavior in the band gap.

In summary, we find that the direct-gap absorption edge in ternary GeSiSn alloys lattice-matched to Ge can be tuned over the 0.8–1.4 eV range. Research in photovoltaics has identified a hypothetical 1-eV gap material lattice-matched to Ge as the most promising route to improve the performance of multijunction solar cells based on the Ge/InGaAs/InGaP system [16,17]. Our alloys meet these two fundamental requirements, and may have important applications in this field. The analysis of the compositional dependence of the direct band gap yields a very rich phenomenology unique to ternary alloys. This includes the coexistence of small and large bowing parameters, which probably implies that the nature of the band-edge states can also be tuned from bandlike to impuritylike by proper adjustment of the alloy composition.

This work was supported by the Air Force Office of Scientific Research under Grant No. FA9550-60-01-0442 (MURI program) and by the Department of Energy under Grant No. DE-FG36-08GO18003. We thank Voltaix Corporation for donating the trisilane used in the growth of GeSiSn.

*vdcosta@asu.edu
†yfang6@asu.edu
‡john.tolle@asu.edu
§john.kouvetakis@asu.edu
‖jose.menendez@asu.edu

[1] L. Nordheim, Ann. Phys. (Leipzig) **401**, 607 (1931).
[2] M. Jaros, Rep. Prog. Phys. **48**, 1091 (1985).
[3] I. Vurgaftman, J. R. Meyer, and L. R. Ram-Mohan, J. Appl. Phys. **89**, 5815 (2001).
[4] D. J. Paul, Semicond. Sci. Technol. **19**, R75 (2004).
[5] S. T. Pantelides and S. Zollner, *Silicon-Germanium Carbon Alloys: Growth, Properties, and Applications* (Taylor & Francis, New York, 2002), Vol. 15, p. 538.
[6] M. Bauer, C. Ritter, P. A. Crozier, J. Ren, J. Menéndez, G. Wolf, and J. Kouvetakis, Appl. Phys. Lett. **83**, 2163 (2003).
[7] P. Aella, C. Cook, J. Tolle, S. Zollner, A. V. G. Chizmeshya, and J. Kouvetakis, Appl. Phys. Lett. **84**, 888 (2004).
[8] V. R. D'Costa, C. S. Cook, J. Menendez, J. Tolle, J. Kouvetakis, and S. Zollner, Solid State Commun. **138**, 309 (2006).
[9] T. Mattila, S.-H. Wei, and A. Zunger, Phys. Rev. B **60**, R11245 (1999).
[10] M. A. Wistey, Y. Y. Fang, J. Tolle, A. V. G. Chizmeshya, and J. Kouvetakis, Appl. Phys. Lett. **90**, 082108 (2007).
[11] C. M. Herzinger, B. Johs, W. A. McGahan, J. A. Woollam, and W. Paulson, J. Appl. Phys. **83**, 3323 (1998).
[12] V. R. D'Costa, C. S. Cook, A. G. Birdwell, C. L. Littler, M. Canonico, S. Zollner, J. Kouvetakis, and J. Menendez, Phys. Rev. B **73**, 125207 (2006).
[13] B. Johs, C. M. Herzinger, J. H. Dinan, A. Cornfeld, and J. D. Benson, Thin Solid Films **313–314**, 137 (1998).
[14] J. Tolle, A. V. G. Chizmeshya, Y. Y. Fang, J. Kouvetakis, V. R. D'Costa, C. W. Hu, J. Menendez, and I. S. T. Tsong, Appl. Phys. Lett. **89**, 231924 (2006).
[15] S. H. Wei and A. Zunger, Phys. Rev. Lett. **76**, 664 (1996).
[16] D. J. Friedman, S. R. Kurtz, and J. F. Geisz, in Photovoltaic Specialists Conference, 2002. Conference Record of the Twenty-Ninth IEEE2002 (IEEE, New York, 2002), p. 856.
[17] F. Dimroth and S. Kurtz, MRS Bull. **32**, 230 (2007).